



**Designers Guide to  
Box Girder Bridges**

**Bethlehem** 

# Designer's Guide to Steel Box Girder Bridges

---

Professor Conrad P. Heins, Jr.  
Civil Engineering Department and  
Institute for Physical Science and Technology  
University of Maryland

Dann H. Hall, Consulting Engineer  
Bethlehem Steel Corporation

---

We wish to express our appreciation to  
C. S. Morgenthaler, Vice President  
and A. Gruver, Chief Bridge Engineer,  
Envirodyne Engineers, Inc., Baltimore, Md.,  
for their consultative services during the  
development and preparation of this booklet.

---

Bethlehem Steel Corporation  
Bethlehem, Pennsylvania

Booklet No. 3500  
Printed in U.S.A.

Data current as of  
February 1981

# Contents

Notations . . . . .	3
Introduction . . . . .	4
Structural Behavior of Box Girders . . . . .	5
Stress Components . . . . .	6
Structural Analysis . . . . .	10
Skewed Bridges . . . . .	11
Shear Lag . . . . .	11
Fatigue . . . . .	12
Number of Cycles . . . . .	12
Diaphragms. . . . .	12
Top Lateral Bracing . . . . .	12
Shear Connectors . . . . .	12
Transverse Stiffeners. . . . .	12
Flange-to-Web Welds . . . . .	12
Vibration . . . . .	13
Beam on Elastic Foundation Analogy . . . . .	13
Design Considerations . . . . .	14
Selection of Steel . . . . .	14
Optimum Box Configuration. . . . .	14
Flange Design . . . . .	15
Web Design . . . . .	15
Splices . . . . .	16
Single-and Multiple-Cell Boxes . . . . .	16
Open Top Box Girders . . . . .	16
Diaphragms . . . . .	17
Box Girder with Floor Beams . . . . .	19
Appendix – Beam on Elastic Foundation Analogy (BEF) for Determining Distortional Stresses in Box Girders. . . . .	20
(BEF) Example . . . . .	26
References . . . . .	31

# Notations

A	= enclosed area of box	q	= diaphragm brace stiffness/box stiffness/length (nondimensional)
$A_b$	= area of one diaphragm bracing member	R	= bridge radius
$A_{flg}$	= bottom flange area	$R_{A,B,C,D}$	= reactions
a	= width of box at top	r	= radius of gyration
Bi	= bimoment (k-in <sup>2</sup> )	S	= section modulus
b	= width of box at base	$S_w$	= warping statical moment (in <sup>4</sup> )
$C_b$	= BEF factor for determining the diaphragm force	T	= concentrated torque
$C_t$	= BEF factor for determining the transverse distortional bending stress	t	= plate thickness
$C_w$	= BEF factor for determining the normal distortional warping stress	V	= shear
c	= inclined height of box	v	= compatibility shear at center of box bottom
D	= transverse flexural rigidity	$V_b$	= bending shear
d	= stiffener spacing	$V_s$	= shear connector force
$d_o$	= effective width of web or flange plate acting with stiffener	$V_{st}$	= Saint-Venant's torsional shear
E	= Young's modulus	W	= bridge weight per length
$E_b$	= Young's modulus of diaphragm bracing	$W_L$	= AASHTO wheel load factor
$F_b$	= force in diaphragm	$W_n$	= normalized warping function (in <sup>2</sup> )
$F_d$	= transverse bending stress in box plate due to an applied torque	$\tilde{W}, A^*, \tilde{S}$	= see References 4 and 12
$F_y$	= minimum specified yield stress	X	= 1/R
$f_b$	= natural frequency (Hz)	x	= distance from a diaphragm
$f'_c$	= minimum specified compression strength of concrete	y	= vertical distance to extreme fiber from neutral axis
G	= shear modulus	$\alpha$	= angle of skew
g	= acceleration of gravity	$\beta$	= BEF stiffness parameter (in <sup>-1</sup> )
h	= box depth	$\gamma$	= distortional angle (radians)
I	= moment of inertia of box section	$\gamma'$	= first derivative of distortion angle
$I_s$	= moment of inertia of stiffener bar and effective portion of web or flange	$\gamma''$	= second derivative of distortion angle
$I_w$	= warping constant (in <sup>6</sup> )	$\Delta_b$	= deflection due to flexure
K	= effective length factor	$\delta_b$	= deformation of bracing member due to applied torque (in <sup>2</sup> /k)
$K_f$	= constant	$\delta_1$	= box distortion per kip per inch of load without diaphragms (in <sup>2</sup> /k)
$K_T$	= torsional constant (in <sup>4</sup> )	$\mu$	= Poisson's ratio
k	= buckling coefficient	$\sigma_b$	= normal bending stress
L	= simple span length	$\sigma_{dw}$	= normal distortional warping stress
$L_b$	= length of diaphragm bracing member	$\sigma_t$	= transverse bending stress
l	= diaphragm spacing	$\sigma_{tw}$	= normal torsional warping stress
M	= in-plane moment	$\tau$	= Saint-Venant shearing stress
m	= uniformly applied torque	$\tau_b$	= bending shear stress
n	= modular ratio	$\tau_{dw}$	= distortional warping shear stress
NB	= number of box girders in the bridge	$\tau_{tw}$	= torsional warping shear stress
P	= load	$\phi$	= angle of rotation
Q	= statical moment (in <sup>3</sup> )	$\bar{\phi}$	= subtended angle between radial piers
		$\psi$	= $L \sqrt{G K_T / E I_w}$

# Introduction

Steel box girder bridges have come into common usage in many countries for a variety of applications since welding has permitted their fabrication with relative ease. Box girders provide aesthetically pleasing uncluttered undersurfaces and reduce the exposed surface needing maintenance. Box girders are 100 to 1,000 times stiffer in torsion than I-girders. This torsional stiffness permits the elimination of many bracing members in

many cases where torsional loading is large. The large torsional stiffness affects the distribution of loads in multibox bridges.

This booklet examines the structural behavior of box bridges and some of the considerations necessary for economical box girder design. Steel boxes not covered by AASHTO provisions, such as transit structures and horizontally curved structures, can be examined using the guides

provided. An appendix presents a summary of the Beam on Elastic Foundation analogy for distortional stresses in box members. A liberal bibliography is included to assist the designer when his needs exceed the scope of this publication.

# Structural Behavior Of Box Girders

Figure 1 shows deformations due to bending and torsional loads on a box girder. Figure 2a shows how a load applied away from the shear center of the box can be separated into bending and tor-

sional components for analysis using superposition. In Figure 2b the torsional load is further separated into pure torsional and distortional components.

**Figure 1/**Box deformations due to vertical and torsional loads

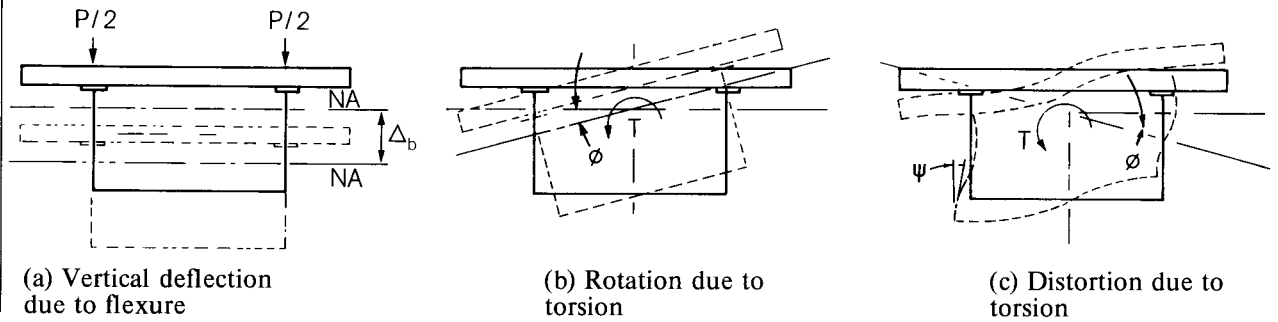


**Figure 2a/**Separation of general loading into bending and torsional components

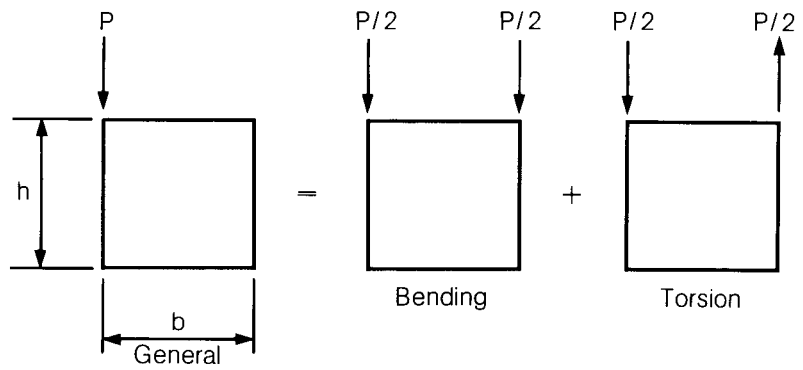
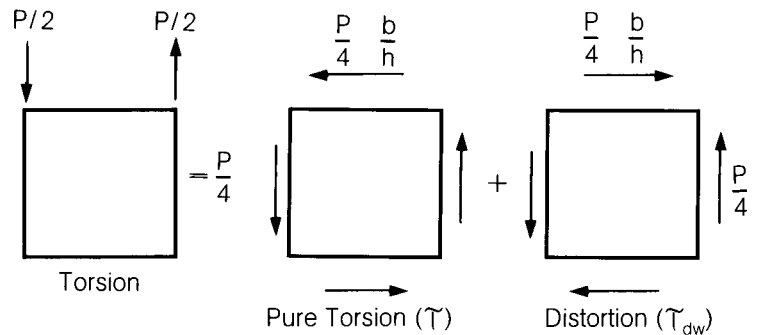


**Figure 2b/**Separation of torsional load into pure torsional load components



## Stress Components

Associated with these flexural and torsional loads are three normal stresses, four shear stresses, and one bending stress through the plate thickness. Typical diagrams for each of these stresses are shown in Figures 3 through 10. The stresses in Figures 3 and 4 are due to bending about the horizontal axis. Figure 5 shows the Saint-Venant shear flow diagram. The shear stress,  $\tau$ , is a function of the box wall thickness and the reciprocal of the enclosed area of the box. Figure 6 shows the normal torsional warping stress. This stress is generally very small in closed box sections and can be ignored. Figure 7 shows the warping shear stress associated with the normal stresses in Figure 6. Figures 8 through 10 represent stress diagrams for the stresses associated with distortion of the box cross section. These stresses were first calculated by Vlasov (27). Dabrowski (4) developed the equations shown with Figures 8 through 10. The stress diagram in Figure 10 is for the stress in the outside fiber of the box components. Dis-

tortional stresses occur because the section is attempting to become more round. If the box were round, distortional stresses would be zero. Distortion stresses are decreased by the addition of diaphragms. Without diaphragms, the distortion stresses may be large if torsion is large.

The equation for the calculation of each stress component is given on the corresponding figure. These equations for torsional behavior are developed in Reference (12). Torsional properties for composite sections are calculated by equations given in References (9) and (10).

Torsional warping stresses in box sections are generally negligible; however, if the section has only three sides (trough boxes) without sufficient top bracing, the torsional warping stresses and rotational deflection before the deck cures may be large. Top bracing of such sections is generally advisable.

**Figure 3**/Normal Bending Stress

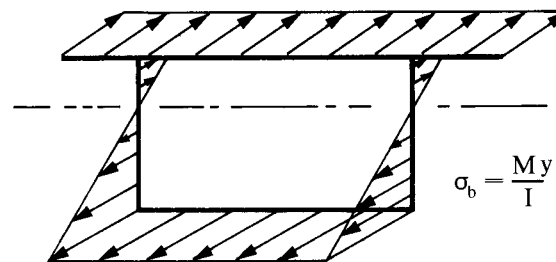


**Figure 4/**Bending shear flow diagram

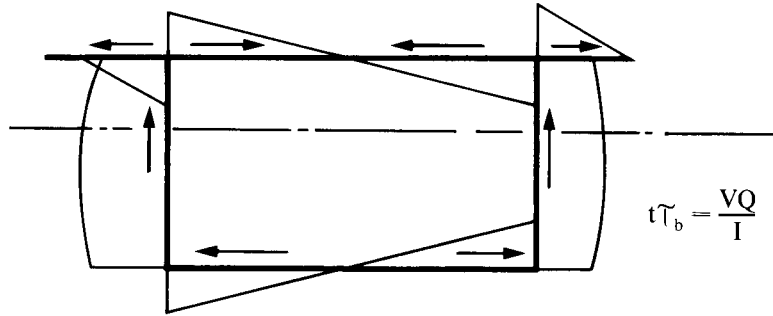


**Figure 5/**Saint-Venant Shear flow diagram

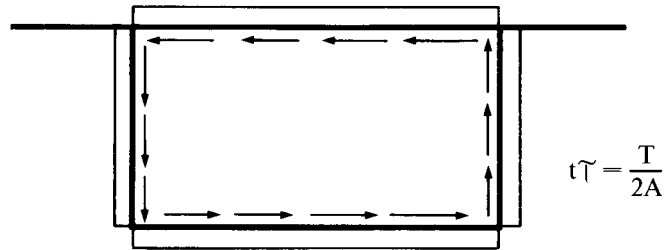


**Figure 6/**Normal torsional warping stress

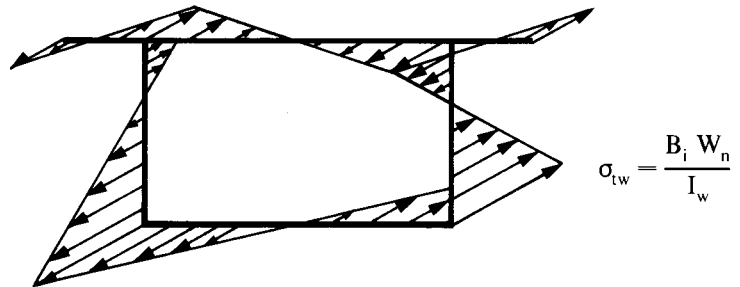


**Figure 7/**Torsional warping shear flow diagram

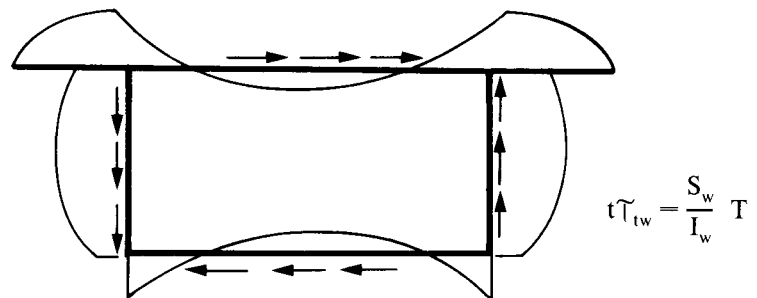


**Figure 8/**Normal  
distortional  
warping stress

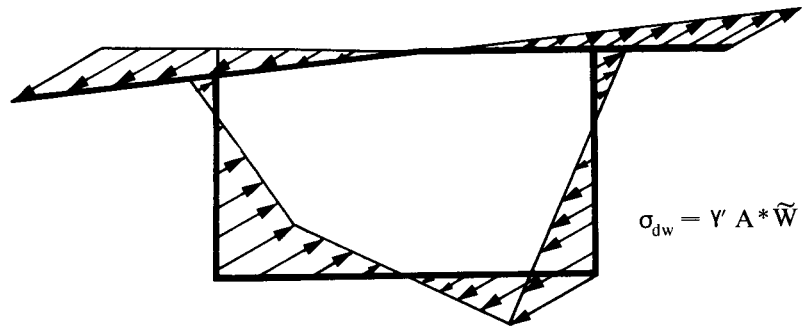


**Figure 9/**Distortional  
warping shear  
flow diagram

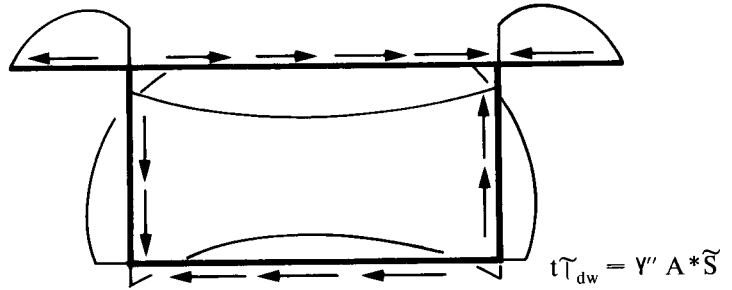
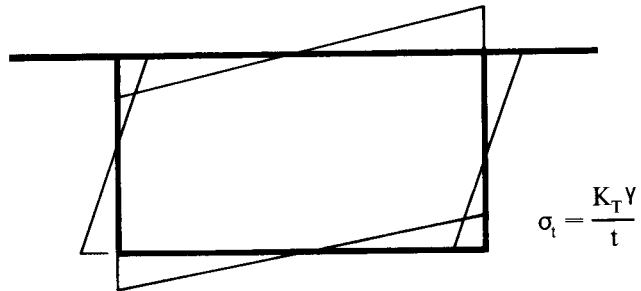


**Figure 10/**Distortional  
transverse bending  
stress diagram



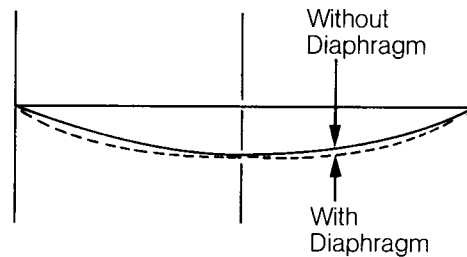
The magnitude of the torsional stresses varies with respect to diaphragm rigidity, diaphragm spacing, and location of torsional load. Figures 11, 12 and 13 show typical influence lines for normal torsional warping stress, normal distortional stress, and transverse distortional bending stress at midpoint of diaphragm spacing, respectively. In Figure 11, the end points of the box are assumed to have rigid diaphragms which do not permit cross-section deformation, but do not restrain box movement in the normal direction. This condition is referred to as torsionally pinned. The effect of a diaphragm added at midpoint is shown by the dotted curve. The added diaphragm provides torsional rigidity, or forbids the movement of the box in the normal direction, or cross section out-of-plane displacement. If a concentrated torque is applied at this diaphragm there is no effect. However, if the torque is applied at some other point, the diaphragm attracts the torque, slightly increasing the normal warping stress at the diaphragm. This situation

might occur at a bearing diaphragm. There are no stress values provided on the ordinates; however, the stresses are generally inconsequential for closed box members.

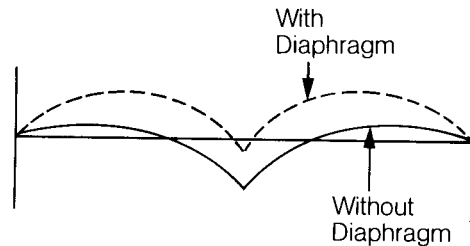
The dashed line in Figure 12 shows the influence on normal distortional stress if a rigid diaphragm is added at midpoint. The diaphragms in this instance need not be torsionally rigid. The addition of the diaphragm reduces the normal distortional stress at the point of the new diaphragm if the torque is applied at the new diaphragm. However, if it is applied at the quarter points of the original panel, the stresses may be as high as without the diaphragm. Thus, normal distortional stresses should be rechecked for various loading conditions after the addition of a diaphragm.

Figure 13 shows the dramatic reduction in distortional transverse bending stress obtained by the addition of a diaphragm. However, it may be necessary to also check these stresses for different load positions.

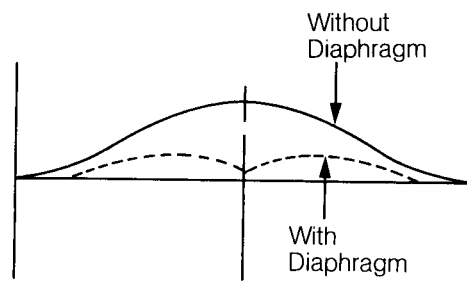
**Figure 11/**Influence line for normal torsional warping stress  $\sigma_{tw}$  at midpanel with ends torsionally pinned



**Figure 12/**Influence line for normal distortional warping stress  $\sigma_{dw}$  at midpanel



**Figure 13/**Influence line for transverse distortional bending stress  $\sigma_t$  at midpanel



# Structural Analysis

The prior discussion tacitly assumed that bending moment and torque were known when examining the behavior of a single box element. Analysis must consider the torsional, as well as flexural stiffness of the box members, so more unknowns must be considered. This makes the problem more complicated than the similar problem of a bridge composed of a deck supported by a series of torsionally weak girders. Analysis of this common I-girder bridge system resulted in the familiar AASHTO wheel load distribution factors which greatly simplify design of multiple girder bridges. The AASHTO Bridge Specifications (Sections 1.7.49 and 1.7.64) give a similar wheel load distribution factor for typical box bridges made up of multiple single-cell boxes—based on work done by Mattock (2,16,17). In this study Mattock found intermediate diaphragms were not needed to control distortional stresses within the parameters specified. The study included spans up to 150 feet. A study by Heins et al reported the approximate torque in simple span curved box bridges with various radii, and spans ranging from 50 to 150 feet with one girder per lane (28). A summary of this work is shown in Figure 14. If fewer girders per lane are used, the torque will increase and, conversely, with more girders per lane, the torque per box will decrease. Several computer programs are available to analyze bridges which are not covered in these categories (3,6,13,14,26). Reference (8) gives a tabulation of available computer programs and their capabilities.

In the analysis of simple span structures with single boxes, such as some transit systems, moments and torques, can be calculated directly.

Single continuous box girders should be examined for additional unknowns introduced where torsion is restrained by the bearings.

One investigation (28) showed that the AASHTO straight box wheel load factor could be modified by the following relationships to provide live load moments and torques for simple span curved box girders:

$$\text{Moment} = [1440 X^2 + 4.8 X + 1] W_L \quad (1)$$

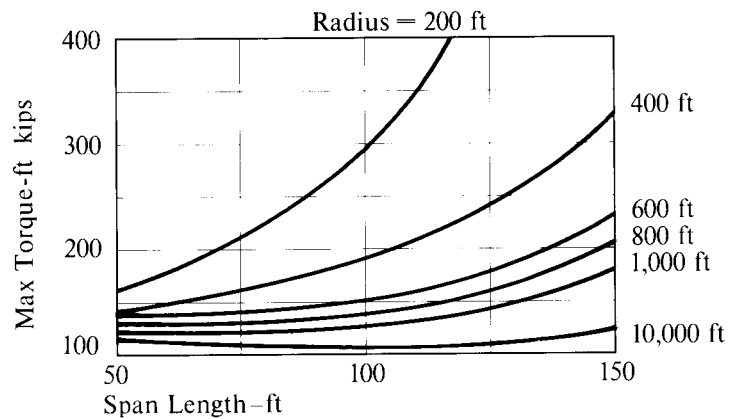
$$\text{Torque} = [18550 X^2 + 50 X] W_L \quad (2)$$

where:  $X = \frac{1}{\text{radius}}$

$W_L = \text{AASHTO wheel load distribution factor.}$

These empirical relationships were developed from studies where the piers were radial with respect to the center of curvature. The wheel load factor is applicable only for bridges without skew.

**Figure 14**/Live load torque for curved box bridges with HS20 loading



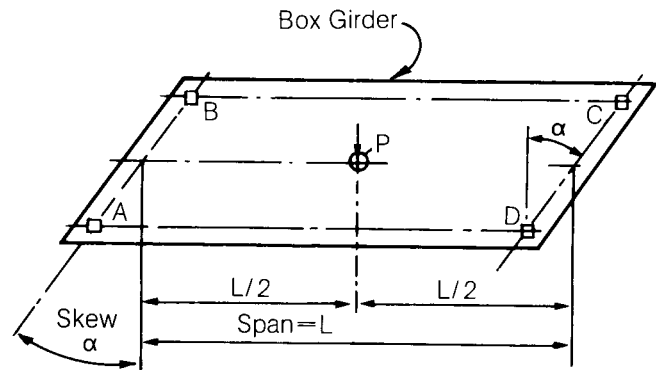
## Skewed Bridges

Skewed bridges are subjected to additional forces. These forces introduce additional moment into the girders and slab which must be considered in design. In the case of box bridges, the increased torsional stiffness can cause additional moments and torques in the box. Figure 15 shows a schematic plan view of a single box with skewed supports and a single load,  $P$ , at the center. Reactions  $R_B$  and  $R_D$  are equal because of symmetry in this example, as are  $R_A$  and  $R_C$ . But more important,  $R_B$  and  $R_D$  are greater than  $R_A$  and  $R_C$ . This difference introduces equal and opposite torques and longitudinal moments at

the ends of the box. As the skew and/or the box width increase, these moments and torques increase.

When piers supporting curved box girders are not perpendicular to the tangent of the girders, a similar effect is experienced. This situation additionally complicates the analysis, and increases the forces the bridge must resist. As a result, designers seem to avoid the situation when possible (7).

**Figure 15/** Plan of skewed box with load "P" at center



## Shear Lag

The first order assumption that plane sections remain plane after bending is not always appropriate with box sections. If a box flange is particularly wide, normal stress in the flange near the webs may be significantly higher than at mid-width because the shear rigidity of the flange is less than the axial rigidity. If longitudinal stiffeners are present, the rigidity of the flange in the longitudinal direction is increased with no increase in the shear rigidity; as a result, shear lag is accentuated.

Moffat and Dowling (19) report the effective width ratio for flexural stress is 0.52 when width/span = 0.2 for a concentrated load and no longitudinal stiffeners. When longitudinal stiffeners are added such that their area equals the area of the flange, the effective width is reduced to 0.40. The concentrated load condition can represent the pier location on continuous spans. With uniform loading, the effect of shear lag is less severe.

The shear lag effect also influences the behavior of longitudinal reinforcement in the slab. The shear transfer between these bars and the girder is by the concrete slab. Cracks in the slab have the effect of reducing the shear rigidity and decreasing the effective width. The result is increased bending stresses. Composite steel and concrete bridges with webs widely spaced may not act as fully composite structures for this reason. The stresses in shear connectors and concrete slab should be examined for this situation in design of composite bridges where the box width exceeds about 16 times the structural slab thickness.

## Fatigue

Welded box girders are subject to more stress components than I-girders, as previously discussed. The additional stresses should be considered in the design, although box girders are not particularly fatigue-critical.

**Number of Cycles**/The normal stress in a box girder is composed of flexural, torsional warping and distortional warping. These stresses will be additive at one location in the cross section. The maximum stress is at a corner of the box.

In straight girders, the sense of torsion may be either positive or negative, depending on the location of the loads with respect to the shear center of the box girder. The fatigue stress can be conservatively calculated as the maximum tensile stress found by superposition of all normal stresses. Transverse bending stresses contribute a normal component due to the Poisson effect. Since superposition applies only for cases when the stress states can exist simultaneously, it is rarely necessary to add all possible stresses.

The possibility of stresses in diaphragm members and associated stresses, as well as distortional transverse bending stresses undergoing full reversal in straight girders exists, but is remote. Most traffic passes within specific lanes, and stress reversal requires alternating trucks to be in alternating critical locations. Engineering judgment must be exercised in such cases. One approach may be to increase the calculated diaphragm or transverse bending stresses by some percentage to account for uncertainty in vehicle location.

**Diaphragms**/In straight multiple girder structures, torsion is small and diaphragm forces are relatively small. However, the force in diaphragm members of boxes can be significant. It is advisable to consider the local effect this force has on the box webs and flanges. Additional, less rigid diaphragms are sometimes needed to reduce thrust forces against the box components.

**Top Lateral Bracing**/Although these members may be ignored in the structural design of trough girders for live load, they may have an effect on the fatigue behavior of the main members (18). If they are fillet welded to the top flange, the flange stresses are limited by Category D or E in AASHTO.

**Shear Connectors**/When torsional loads are significant, the additional force due to Saint-Venant shear should be vectorially added to the shear connectors. It has been found that the torsional warping shear and the distortional warping shear are not significant (24). Thus, the shear connector force,  $V_s$ , is found by Equation 3:

$$V_s = \sqrt{V_b^2 + V_{st}^2} \quad (3)$$

where  $V_b$  = bending shear

$V_{st}$  = Saint-Venant torsional shear

**Transverse Stiffeners**/The stress concentration at the end of transverse stiffeners, due to distortional transverse bending stresses in the web or flanges, can be substantial. The web stiffeners often are not welded to the flanges, causing very high local stresses at the end of the stiffeners. If the transverse stiffeners are welded to the flanges, the welds, as well as the base material stressing are reduced substantially. The base metal fatigue stress would be controlled by AASHTO Category E in either case. In the first case, moment is resisted only by the web. In the second case, the stiffener helps transfer moment into the flange, mitigating the strain concentration. Category F should be used for the stiffener welds. This discontinuity can be improved further by the addition of transverse flange stiffeners attached to the transverse web stiffeners. Ideally, avoidance of these transverse stiffeners by increasing the web thickness is most desirable. In high shear regions with large torsion, closely spaced diaphragms will reduce box distortion and associated stresses.

**Flange-to-Web Welds**/Fillet welds on both sides of the web provide more resistance to distortion of the box corners than single side welds which can develop high strains. If torsion is nominal—as is the case with box girders within AASHTO parameters—single side welding is usually satisfactory. A full-penetration flange-web weld is sometimes specified (7), but is generally not necessary.

## Vibration

Vibration of girders in rapid transit systems has received much attention, and most transit criteria specify a minimum fundamental frequency for flexure. The fundamental frequency of a simple span bridge is given by Equation 4:

$$f_b = \frac{\pi}{2L^2} \sqrt{\frac{E \times NB \times I \times g}{W}} \quad (4)$$

where:  $L$  = span length  
 $W$  = bridge weight per length  
 $g$  = acceleration of gravity  
 $NB$  = number of boxes  
 $E$  = Young's modulus  
 $I$  = moment of inertia of one box

When  $f_b$  greater than  $\pi$  is required:

$$NB \times I > \frac{4L^4 W}{E g} \quad (5)$$

The moment of inertia is a function of girder depth squared, and the flange areas. An approximate relationship for required depth,  $h$ , based on the above assumptions is given by Equation 6:

$$h = K_r \times L^2 \sqrt{\frac{W}{A_{flg} \times NB \times E \times g}} \quad (6)$$

where:  $A_{flg}$  = area of bottom flange

$K_r$  = constant which is a function of the ratio of top to bottom flange areas

The torsional vibration mode of box members may be significant. This analysis is presented in Reference (6).

## Beam on Elastic Foundation Analogy

Distortional stresses in box beams may be examined, using the Beam on Elastic Foundation (BEF) analogy first discussed by Vlasov (27), and extended by Abdel-Samad, Wright, et al (1,30,31), and later by Williamson (29). The accuracy of this analogy has been confirmed by tests (20). In the analogy the diaphragms, or trans-

verse cross bracing, are analogous to intermediate supports in the BEF, and the resistance to distortion provided by the box cross section is analogous to a continuous elastic foundation. A discussion of this analogy and an example using certain charts is contained in the Appendix.

## Design Considerations

Torsionally induced forces and wide-flange plates cause the proportioning of box girders to be somewhat more complex than I-girders. In single box, or horizontally curved box structures torsion is a significant factor, and distortion of the box may cause significant stresses in the box.

However, as the BEF charts indicate, addition of diaphragms significantly reduces the box stresses due to distortion so that box components can generally be proportioned for flexural stresses with no more than 10 percent allowance for normal stresses due to torsion.

### Selection of Steel

Significant economies can be realized by judicious selection of steels. The most commonly used grades in bridge construction are all candidates for box construction. A recent survey showed that weathering steel is probably the most commonly used steel in U.S. box bridges. It combines high design stresses with minimal maintenance cost, providing much the same economies designers realize in I-girder bridges.

The bottom flange is generally stiffened longitudinally in compression regions. Therefore, the higher strength of weathering steel can usually be mobilized with little or no additional fabrication beyond that for carbon steel. One cost comparison from several fabricators of a rapid transit system showed the average prices of

ASTM-A588 weathering steel box girders to be about 5 percent less than a similar, painted ASTM-A36 design. As in many transit systems, the girders were simple span.

Short- to medium-span continuous box bridges are generally kept at a constant depth to simplify fabrication of the boxes. Thus, the optimum depth is a compromise between the optimum depth at the piers and at midspan. The location of piers is often fixed by other constraints, and in the case of box girders, the flange width is constant.

### Optimum Box Configuration

Optimizing the box configuration includes selecting the number of boxes, their depth, and width. Span ratios can affect the box configuration, and should be varied in conjunction with selecting proportions for the boxes.

If the design is to meet present AASHTO (1980) requirements, the ratio of box width to lane width,  $R$ , is limited to 1.5. The wheel load distribution factor per box is reduced as the box width is increased. The opposing factor to wide boxes is effective use of the flange material. Particularly in continuous bridges, shear lag should be considered at the pier locations if the web spacing is greater than five times the distance between points of contraflexure. Longitudinal flange stiffening can mobilize the full flange area in compression, but excessive stiffening is expensive and contributes to the shear lag. Inclined webs provide more uniformly spaced support for the slab in conjunction with a narrower bottom flange. The cost of inclined webs for tangent girders with constant depth is not significantly different from girders with rectangular cross sections.

Optimal box depth is, perhaps, more critical for box girders than I-girders because the flange size can be varied less over the bridge length. Figure 2b shows that, for vertical loads applied at the sides of a box, shear is proportional to the box width and inversely proportional to the box depth; thus, boxes that are overly shallow have high shear forces. The optimal depth of I-girders is often a good starting point in optimizing the box depth.

## Flange Design

Longitudinal flange stiffening in compression flanges is suggested by AASHTO if  $b/t$  exceeds 60. However, many designers use longitudinal stiffeners when  $b/t$  exceeds 45 (7). When designed by AASHTO, longitudinal stiffeners are proportioned by a stiffness criterion which controls the buckling of the flange plate. The stiffness is a function of the plate buckling coefficient,  $k$ .

When  $k=4.0$ , the stiffeners are sufficiently rigid to force plate buckling between the stiffeners. When  $k$  is less than 4.0, the rigidity of the stiffeners is reduced so that they will not form nodal points for plate buckling, and buckling of the stiffeners will occur. The required size of stiffeners increase as their spacing decreases because the panel becomes smaller, thus increasing the buckling stress of the panels.

There is no consideration in AASHTO for overall buckling of the longitudinal stiffener as a column. This mode of failure usually is not critical because of the short negative moment region. However, AASHTO provisions recommend a transverse stiffener be placed at the point of dead load contraflexure, which stabilizes the longitudinal stiffeners. If the longitudinal stiffeners become slender and the flange is wide, the engineer may wish to examine overall column buckling of the stiffener. The AASHTO

working stress provisions permit the use of transverse flange stiffeners in conjunction with longitudinal stiffeners designed with  $k=4.0$ . Timoshenko and Gere (25) present a more exhaustive discussion on elastic buckling of stiffened plates.

The most common type of longitudinal flange stiffener is an inverted tee section which provides the desired stiffness with minimum material. The potential of lateral torsional buckling is minimal with structural tee stiffeners. Lateral torsional buckling would be a consideration with an unsymmetrical stiffener such as an angle, although angles are used to stiffen box flanges—particularly in Europe. Bars are also frequently used for longitudinal stiffeners where minimal flange stiffening is needed.

Longitudinal stiffeners are generally not required on tension flanges. However, erection of the members may cause temporary compression stresses in regions where the design stresses are tensile. Stiffeners may be desirable in these cases. Full-length longitudinal stiffeners also eliminate termination of the stiffeners where allowable fatigue stresses are a constraint.

## Web Design

The shear forces in box girders often are similar to those in I-girder bridges, because the number of webs is often similar and the torsional shear forces are often negligible. In other cases such as boxes with inclined webs, or wide boxes where the number of webs is reduced and the torsional loads increased, shear forces become significantly larger than found in I-girders.

Information on size availability of plates from the mills and size price premiums helps to avoid selection of web plates requiring unnecessary shop splices or price extras because of size. Often it is beneficial to change plate thickness if a shop splice is needed. Otherwise, addition of a shop splice for the purpose of changing web thickness is rarely economical.

The question of stiffening a thinner plate vs. a heavier plate with few stiffeners often complicates web design. Fabricators find that, due to more intense fabrication, stiffeners cost about six to eight times web material on a weight basis. Thus, a pound of stiffener should save at least six pounds of web, to be economical. This trade-off often provides the designer with a series of web thicknesses from which to choose, but some fundamental rules of thumb have been found to generally apply. If  $h/t$  is less than 170, longitu-

dinal stiffeners are not required by AASHTO. If  $h/t$  does not exceed 150, transverse stiffeners may be omitted entirely when the shear stress is

less than  $\frac{5.625 \times 10^7}{(c/t_c)^2}$  by AASHTO.  $c$  is inclined

height of box, and  $t_c$  is the web thickness. If torsion is small, the decision of web stiffening is an economic one. The  $c/t_c$  limit of 150 for webs without transverse stiffeners tends to penalize high-strength webs by not permitting the design to use the increased shear strength available. This is one of the reasons hybrid flange-web girders are economical.

Economy is often gained by selecting a web depth which is maximum for the web thickness examined because plate material comes in discrete thicknesses. For example, if a  $c/t_c$  of 150 is desired and the web thickness is 9/16 inch (.5625 in.), the optimum web depth is 150 (.5625)  $\approx$  84 inches.

## Splices

Welded shop splices of box girders are generally more economical than shop bolted splices. Full-penetration shop welds are used, and radiographic inspection is required by AASHTO. Because of the wider flanges, welding and radiographic costs are somewhat higher than for I-girders. As a result, it is often desirable to splice box girder flanges less frequently than I-girders.

Field splices are located in much the same manner as I-girders. They are sometimes welded to provide a smooth appearance, and this method

has been found to be competitive with bolting. However, bolting has other advantages. For example, if longitudinal stiffeners are used in the compression flange of continuous girders, they can be discontinued at the centerline of a bolted splice without concern for fatigue because the stress at the terminus is zero. Bolting also eliminates the need to predict change in camber due to field welding.

## Single- and Multiple-Cell Boxes

A multiple-cell box girder bridge consists of a single box with a series of webs. The webs reduce the shear lag that can occur in the flanges. They also share the shear forces. These

bridges are most economical for very long spans. The use of common bottom flange is effective in creating more equal deformations between adjacent girders, and thus better load distribution (15).

## Open Top Box Girders

Many box girders are built using three steel sides, with the composite concrete deck completing the box enclosure. These are often referred to as "trough-type" or "bathtub" girders. If the top flanges are unbraced, they are subject to lateral torsional instability before the concrete deck has hardened. Therefore, cross bracing as shown in Figure 16 is desirable. One investigation showed that, to cause the box to act as a closed section, the required cross sectional area of the bracing equals  $.03 \times (\text{box width})$  if the diagonal bracing is at 45 degrees. Perpendicular bracing is not effective in shear transfer between the top flanges. The slenderness ( $L_b/r$ ) of bracing members should be less than 100.

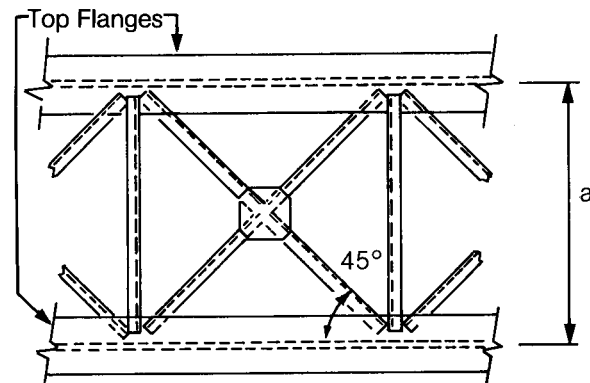
Permanent steel deck forming can be used for top lateral bracing if forms are properly connected to the flanges (11). This may be economi-

cal when compared to the fabrication of bracing members.

Top bracing may be eliminated in some cases by introducing intermediate diaphragms which will prevent lateral buckling of the top flanges in conjunction with a torsionally rigid diaphragm which will prevent warping of the trough prior to curing of the deck. These girders do not provide the same torsional rigidity as boxes with top lateral bracing and are not adequate for curved girders where torsional forces are large.

Open top box girders should not be considered impervious to moisture, and the inside should be protected, or weathering steel used. Provision for inspection of the interior is also desirable.

**Figure 16**/Schematic of typical top bracing for trough box girder

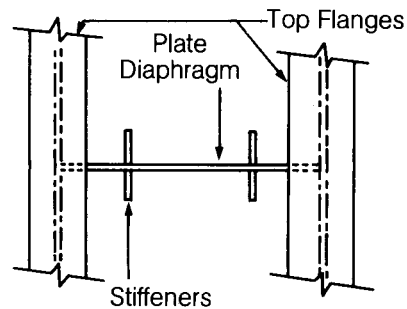


## Diaphragms

Diaphragms prevent distortion of the box, causing an increase in the ability of the box to distribute loads transversely and reduce both normal and transverse distortional stresses.

Diaphragms which are rigid in the normal direction of the box, as shown in Figure 17, will cause an increase in the warping rigidity of the box. This type of diaphragm does not provide a significant benefit to the behavior of the box girder.

**Figure 17**/Internal diaphragm providing warping restraint



For curved box designs, Equation 7 provides diaphragm spacing,  $l$ , which limits normal distortional stresses to about 10 percent of the bending stresses (22,23) for dead load and HS 20 loading:

$$l \leq L \sqrt{\frac{R}{200L - 7500}} \leq 25 \quad (7)$$

where:  $R$  = bridge radius, ft  
 $L$  = simple span length, ft

This equation can be used for cases with one or more boxes per lane and radial piers. For other conditions, a computer analysis which includes distortional effects should be considered. The BEF charts in the Appendix can be used to aid in determining diaphragm requirements.

Studies show that the area of the cross bracing,  $A_b$ , in diaphragms need not be greater than that given in Equation 8, which provides a "q" greater than 1000 (29). The value of q is the relative distortional resistance per inch of length of box:

$$A_b = 750 \left[ \frac{la}{h^2} \right] \left[ \frac{t^3}{(h+a)} \right] \quad (8)$$

where:  $t$  = the thicker plate, either flange or web  
 $l$  = diaphragm spacing  
 $h$  = box height  
 $a$  = width of box at top

Many studies have indicated that box members have properties such that some torsional component stresses may be neglected. The parameter,  $\psi$ , determined by Equation 9, will permit the designer to determine which torsional stresses need be considered:

$$\psi = L \sqrt{GK_T/EI_w} \quad (9)$$

where:  $G$  = shear modulus  
 $K_T$  = torsional constant  
 $I_w$  = warping constant

When  $\psi$  is less than 0.4, evaluation of stresses due to pure warping torsion may be omitted; however, torsional distortion must be considered. When  $\psi$  is greater than 10, evaluation of stresses due to torsional distortion may be omitted; pure torsion must be considered. For curved multiple-box girder bridges,  $\psi$  must have the following values if torsional warping is to be neglected (21):

$$\psi \geq 10 + 40 \bar{\phi} \quad \text{for } 0 \leq \bar{\phi} \leq 0.5 \text{ and}$$

$$\psi \geq 30 \quad \text{for } \bar{\phi} \geq 0.5$$

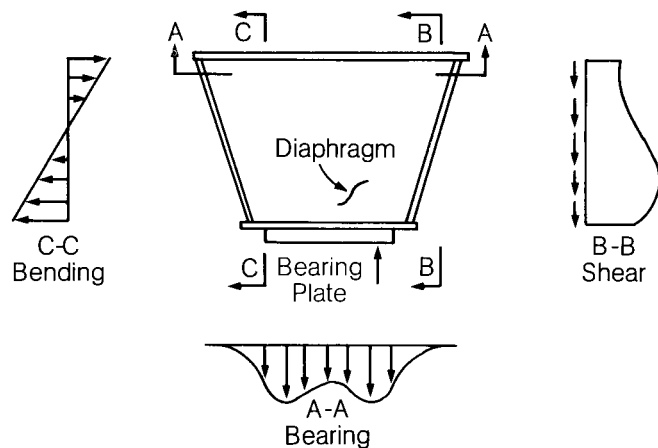
where:  $\bar{\phi}$  = subtended angle (radians) between radial piers

Figure 17 shows a solid plate diaphragm with stiffeners. These stiffeners may cause restraint in the normal direction, inducing increased bimoment in the box. Bimoment or bending across the flanges is caused by either applying a varying torque or varying torsional restraint of the member which will forbid uniform torsional shear stresses. A torsionally stiff diaphragm can substantially vary the torsional stiffness of the box.

Figure 18 shows some of the forces applied to a plate diaphragm at a reaction. The deep beam bending in the diaphragm is accentuated by the centrally located bearing and trapezoidal cross section of the box. The deep beam bending introduces transverse compression stress in the bottom flange of the box. Bearing stresses are also present in the bottom flange. The Poisson effect on these actions causes additional longitudinal compressive stresses which should be added to the bending stresses at interior supports. The flange capacity can be checked by a yield criterion.

Intermediate diaphragms are often cross-brace diaphragms composed of angles attached to transverse stiffeners. The effect of these diaphragms is dependent on their axial stiffness which prevents distortion of the box cross section. It is generally good design practice to include a large number of diaphragms with less stiffness than a few very rigid diaphragms. Rigid diaphragms, widely spaced, may introduce undesirable large local forces into the sides of the box. They can be designed using the BEF charts in the Appendix.

**Figure 18/** Stresses in plate diaphragm at bearing (Ref. 5)



## Box Girders With Floor Beams

Figure 19 shows one alternative to the typical multibox girder structure. In this instance, the floor beams transfer the loads to the main box girders. The floor beams are connected at internal diaphragms within the boxes. The slab can be designed as composite in two directions, and reinforcement placed for two-way action. The AASHTO wheel load distribution factor for box girders is not appropriate. Since torsion is not significant, a grid analysis without distortion or torsional warping may be satisfactory for design.

There are several advantages of such a scheme:

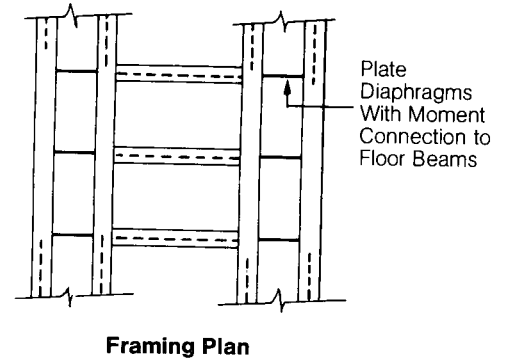
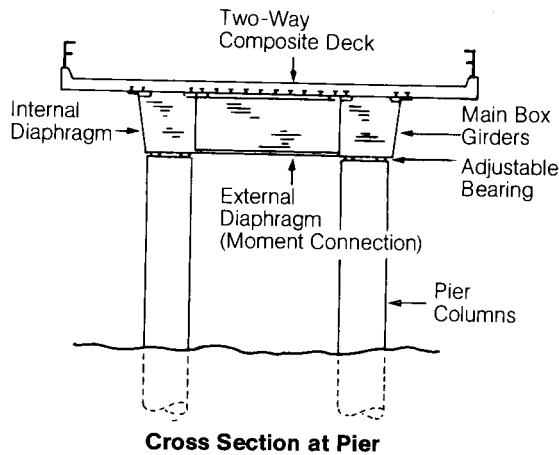
1. Smooth appearance of bridge-pier interface
2. Effective use of bottom flange material throughout the span
3. Avoids forming and casting pier cap
4. Reduces number of main girders, bearings, and splices

5. Each girder is designed for more total load, so a single truck produces proportionately less stress than in a multi-girder bridge, and fatigue is less critical on the box members. Reduction for simultaneous loading of multiple lanes under AASHTO Section 1.2.9 may bring about additional economy.

Disadvantages of the scheme are:

1. There is an increase in the reinforcement in the deck, and forming of the deck is more expensive. However, prestressed concrete deck panels may be used as composite forms to minimize deck costs.
2. The depth of the structure may need to be increased because of the greater moment per main member.
3. The number of fabricated pieces may be increased.

**Figure 19/** Typical steel 2-box system with external diaphragms



# Appendix

## Beam on Elastic Foundation Analogy for Determining Distortional Stresses in Box Girders

This presentation is based on work performed at the University of Illinois under the direction of R. N. Wright, and sponsored by the American Iron and Steel Institute. The example is also taken from this work, with minor modifications.

The deflection,  $\delta_1$ , shown in Figure A1c is due to a torsional load shown in Figure A1a. Deflection,  $\delta_1$ , is the reciprocal of the torsional stiffness of the box, and analogous to the reciprocal of the foundation modulus in the BEF problem. It is computed as follows:

$$\delta_1 = \frac{ab}{24(a+b)} \left\{ \frac{c}{D_c} \left[ \frac{2ab}{a+b} - v(2a+b) \right] + \frac{a^2}{D_a} \left[ \frac{b}{a+b} - v \right] \right\} \quad (\text{A1})$$

where:

$$v = \frac{\frac{1}{D_c} [(2a+b)abc] + \frac{1}{D_a} [ba^3]}{(a+b) \left\{ \frac{a^3}{D_a} + \frac{2c(a^2+ab+b^2)}{D_c} + \frac{b^3}{D_b} \right\}} \quad (\text{A2})$$

$v$  = compatibility shear at center of bottom flange

$$D_a = Et_a^3 / 12 (1 - \mu^2) \quad (\text{A3a})$$

$$D_b = Et_b^3 / 12 (1 - \mu^2) \quad (\text{A3b})$$

$$D_c = Et_c^3 / 12 (1 - \mu^2) \quad (\text{A3c})$$

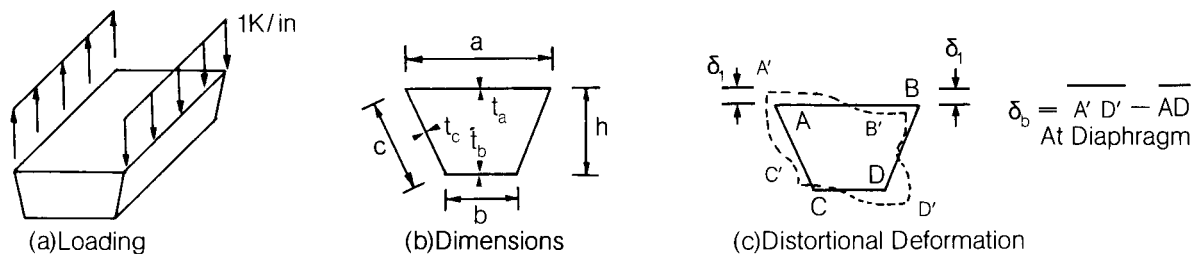
} transverse flexural rigidity of an unstiffened plate ( $k\text{-in}^2/\text{in}$ )

where:  $t_a, t_b, t_c$  = top flange, bottom flange, and web thickness in.  
 $\mu$  = Poisson's ratio

The term,  $v$ , is the compatibility shear at the center of the bottom flange when unit loads are applied at the top corners of the box section of unit length as shown in Figure A1a. The center

of the bottom flange was chosen by Wright (30) because the transverse bending moment and thrust are zero at this point. Dimensions used in Equation 8 are shown in Figure A1b.

**Figure A1/Box under uniform torsional loading**



When transverse stiffeners are present on either flanges or webs, they should be considered in calculating transverse flexural rigidities. The rigidity of the stiffened plate is calculated as follows:

$$D = \frac{EI_s}{d} \quad (\text{A3d})$$

where:  $I_s$  = moment of inertia of stiffened plate  
 $d$  = stiffener spacing

The effective width of plate,  $d_o$ , acting with a stiffener can be determined as follows:

$$d_o = \frac{d \tanh(5.6 d/h)}{\frac{5.6 d}{h} (1 - \mu^2)} \quad (\text{A4})$$

where:  $h$  = transverse length of element,  
 "b" or "c"

Equation A4 is a semiempirical relationship which Wright et al found to give reliably accurate results (30).

The BEF stiffness parameter,  $\beta$ , in the analogy is calculated as follows:

$$\beta \approx \sqrt[4]{\frac{1}{EI\delta_1}} \quad (\text{A5})$$

where:  $I$  = moment of inertia of the box section

Stiffness parameter,  $\beta$ , is a measure of the torsional stiffness of the beam, and is analogous to the beam-foundation parameter in the Beam on Elastic Foundation problem. The diaphragms in the box girder restrict box deformation, and are analogous to supports in the BEF. They are incorporated in the solution by the term "q", which is the dimensionless ratio of diaphragm stiffness to the box stiffness per unit. It is defined as follows:

$$q = \left[ \frac{E_b A_b}{L_b l \delta_1} \right] \delta_b^2 \quad (\text{A6})$$

where:  $E_b$  = Young's modulus of diaphragm material  
 $A_b$  = cross-sectional area of one diaphragm bracing member  
 $L_b$  = length of diaphragm brace

$$\delta_b = \frac{2(1 + a/b)}{\sqrt{1 + \left[ \frac{a+b}{2h} \right]^2}} [\delta_1] \quad (\text{A7})$$

where:  $\delta_b$  = deformation of the bracing member (see Figure A1c)

Equation A6 tacitly assumes that cross bracing is effective in both compression and tension. If the bracing slenderness is large, the bracing is only effective in tension, and  $A_b$  in Equation A6 should be one-half the area of one brace.

The stresses derived from distortion of the box can be determined analogously by solving the BEF problem. Moment in the BEF is analogous to normal distortional stress,  $\sigma_{dw}$ , and deflection in the BEF is analogous to distortional transverse bending stress,  $\sigma_t$ . The reactions in the BEF are analogous to the forces in cross bracing,  $F_b$ . Solutions for these three components are presented in graphical form in Figures A2 through A10. These figures give a "C" value which is used in appropriate equations—A8, A10, A11. These graphs show relationships for uniform torque,  $m$ , or concentrated torque,  $T$ , at midpanel or diaphragms. The figures give the appropriate "C" values for a given box geometry,  $\beta$ , loading, diaphragm stiffness,  $q$ , and spacing,  $l$ . The designer is able to determine the distortion-related stresses, and estimate how diaphragm spacing and stiffness may be best modified if necessary.

Equation A8 gives transverse bending stresses at the top or bottom corners of the box section, depending on the determination of  $F_d$  in Equations A9a and A9b. The critical stress may be in either the web or flange. The AASHTO Specification limits the range of the transverse bending stresses to 20,000 psi. Therefore, the torsion in both directions often must be determined. The stress range is the sum of absolute values of stresses due to opposite torques.

$$\sigma_t = C_t F_d \beta \frac{1}{2a} (ml \text{ or } T) \quad (\text{A8})$$

where:  $m$  = uniform torque per unit length  
 $T$  = concentrated torque

$$F_d = \frac{bv}{2S} \text{ for bottom corner of box} \quad (\text{A9a})$$

$$F_d = \frac{a}{2S} \left( \frac{b}{a+b} - v \right) \text{ for top corner of box} \quad (\text{A9b})$$

where:  $S$  = section modulus of transverse member (see Figure A1c)

Equation A10 gives the normal distortional warping stress at any point in the cross section. The value of  $C_w$  is obtained from either Figures A2, A3 or A9.

$$\sigma_{dw} = \frac{C_w y}{I \beta a} \quad (m\ell \text{ or } T) \quad (\text{A10})$$

where:  $y$  = distance from the transverse vertical axis of the box point under consideration

Equation A11 gives the axial force due to distortional forces applied to the box. The value of  $C_b$  is obtained from either A5 or A10.

$$F_b = C_b \left[ \frac{\sqrt{1 + \left(\frac{a+b}{2h}\right)^2}}{2(1+a/b)} \right] \frac{(m\ell \text{ or } T)}{a} \quad (\text{A11})$$

Since only two loading positions for concentrated loads are considered in the charts, it is often necessary to interpolate between figures. The principle of superposition applies for more than one torque. Figure A11 shows the effect of  $\beta$  on the influence line for diaphragm forces when the diaphragm is rigid.

**Figure A2/**Uniform torque on continuous beam—normal distortional warping stress at midpanel

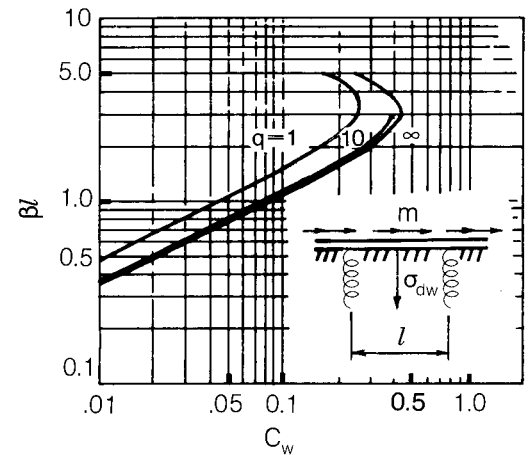


**Figure A3/**Uniform torque on continuous beam. Normal distortional warping stress at diaphragm

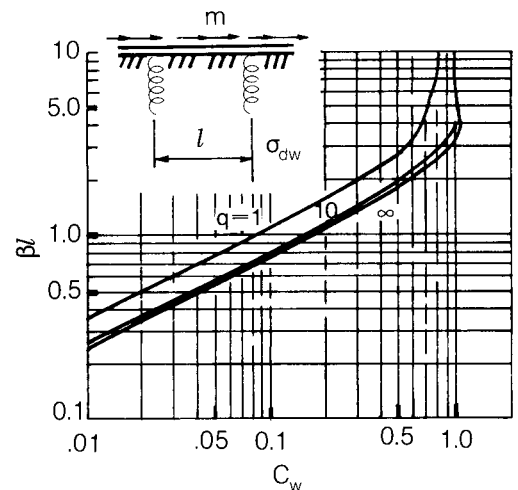


**Figure A4/**Uniform torque on continuous beam—distortional transverse bending stress at midpanel

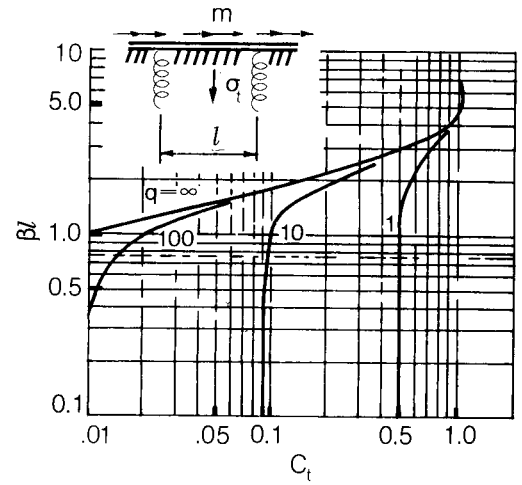


**Figure A5/**Uniform torque on continuous beam—diaphragm force

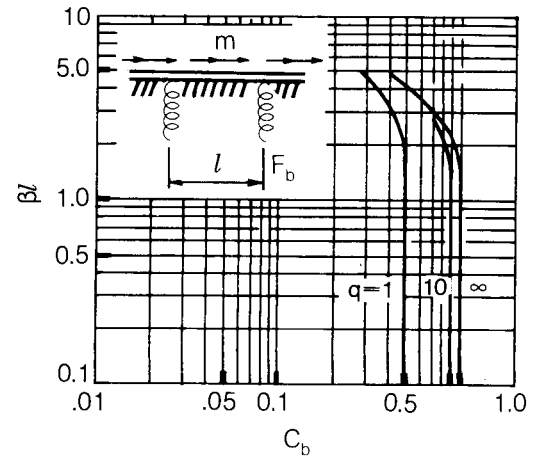


**Figure A6/**Concentrated torque at midpanel on continuous beam—distortional transverse bending stress at load

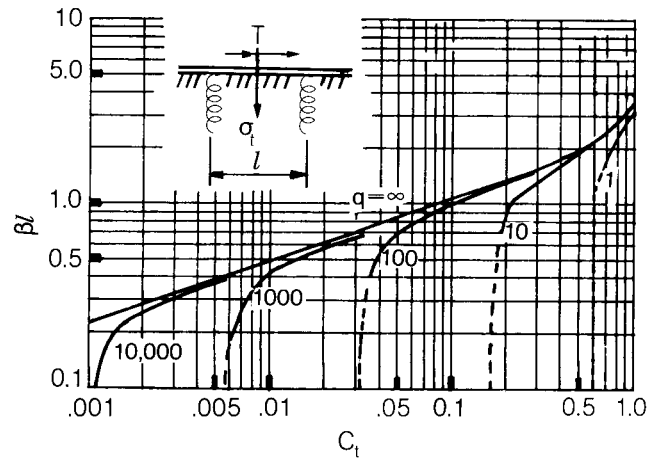


**Figure A7/** Concentrated torque at midpanel on continuous beam—distortional transverse bending stress at diaphragm

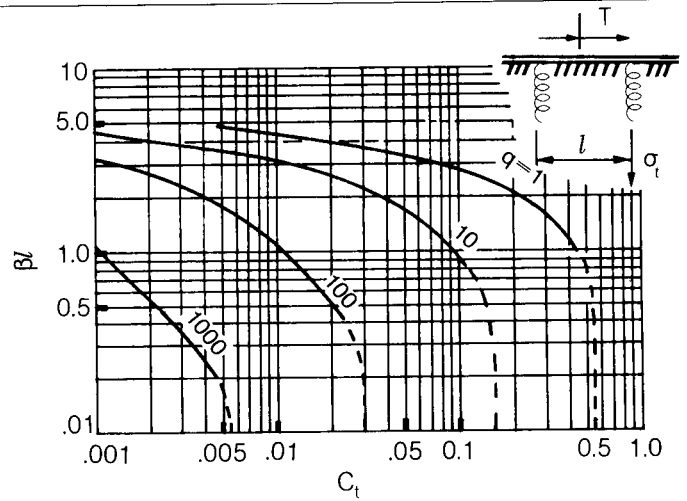


**Figure A8/** Concentrated torque at diaphragm on continuous beam—distortional transverse bending stress at diaphragm

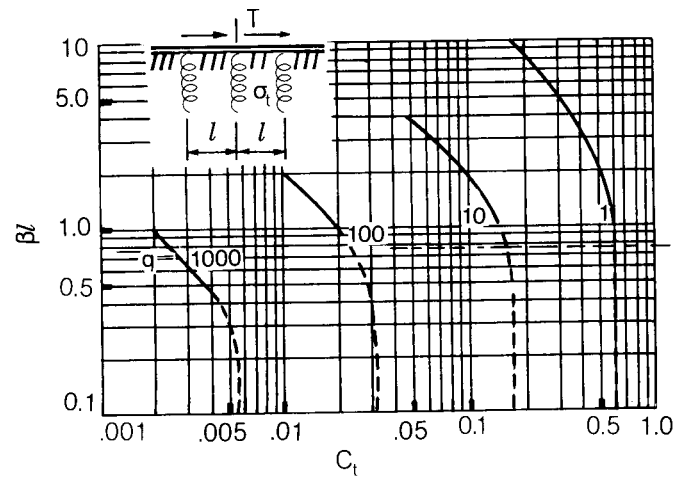


**Figure A9/** Concentrated torque at midpanel on continuous beam—normal distortional warping stress at midpanel

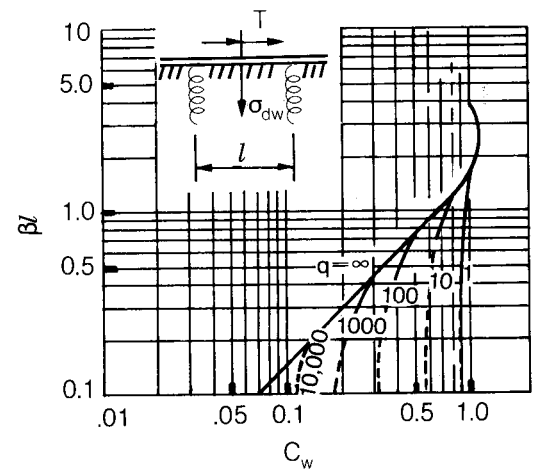


**Figure A10/**Load at diaphragm on continuous beam—diaphragm force

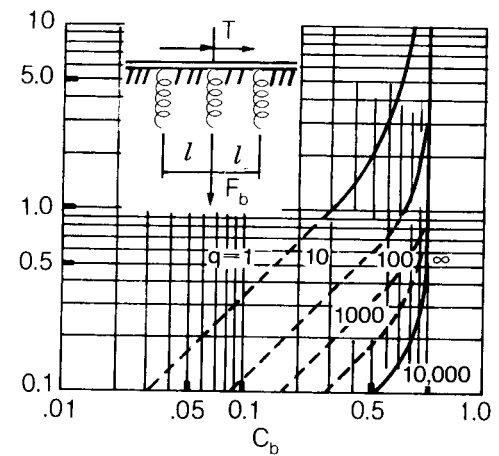
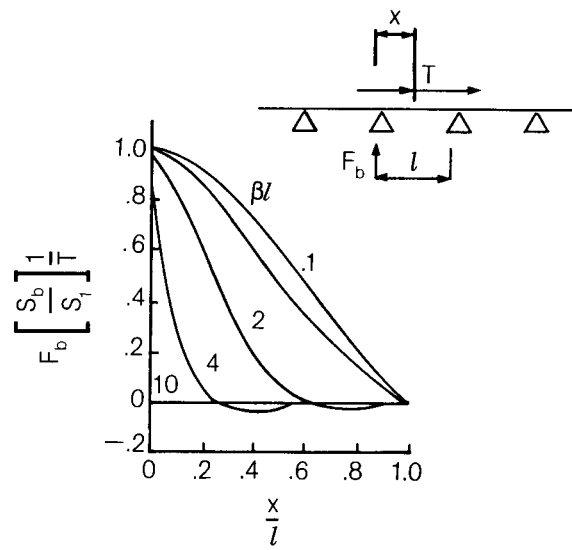


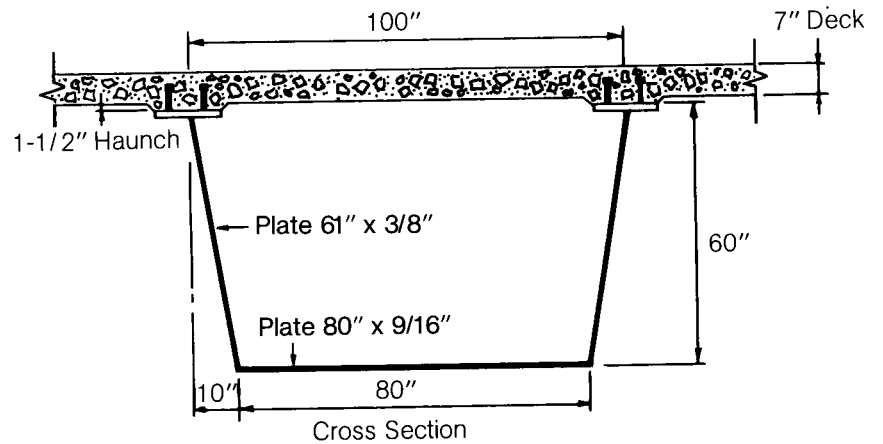
**Figure A11/**Influence line for rigid diaphragm with concentrated torque



### BEF Example

To demonstrate the use of the BEF charts, a short example is presented. Final member sizes and design torques are assumed given, for brevity. Pertinent properties are given in Table 1 and Figure A12. This example is based on data in Reference (30). The torsional load due to a single axle is assumed to be 2000 k-in.

**Figure A12**



Transverse web stiffeners: Bar 6" x 3/8" one side of web  
 Diaphragm spacing: 300 in.  
 Stiffener spacing: 60 in.

**Table 1-Section Properties**

	Units	Midspan	From Equation
I	in <sup>4</sup>	1.90 x 10 <sup>5</sup>	
y <sub>top</sub>	in.	15.41	
y <sub>bottom</sub>	in.	49.59	
v		.058	(A2)
δ <sub>1</sub>	in <sup>2</sup> /k	.822	(A1)
δ <sub>b</sub>	in <sup>2</sup> /k	1.285	(A7)
β	in <sup>-1</sup>	3.84 x 10 <sup>-3</sup>	(A5)
S <sub>web</sub>	in <sup>3</sup> /in	7.16 x 10 <sup>-2</sup>	
F <sub>d</sub> (top corner critical)	in <sup>-1</sup>	270	(A9a) (A9b)

Steel:  $F_y = 36$  ksi  
 $E = 29,000$   
 $\mu = 0.30$

Concrete:  $f'_c = 4,000$  psi  
 $n = 8$   
 $E = 3625$  ksi  
 $\mu = 0.30$

$$I_{\text{composite}} = 190,000 \text{ in}^4$$

$$D_a = \frac{Et_a^3}{12(1 - \mu^2)} \quad (\text{A3a})$$

$$D_a = \frac{3625 \times 7^3}{12(1 - .3^2)} = 114,000 \text{ k-in}^2/\text{in}$$

Find effective width of plate at transverse stiffeners.

$$d_o = \frac{d \tanh(5.6 d/h)}{\frac{5.6 d}{h} (1 - \mu^2)} \quad (\text{A4})$$

$$d_o = \frac{60 \tanh(5.6) (60/60)}{\frac{5.6(60)}{60} (1 - .3^2)} = \underline{\underline{11.8 \text{ in.}}}$$

Effective rigidity of web with transverse stiffener

$$I_s = 22 \text{ in}^4$$

$$D_c = \frac{EI_s}{d} = \frac{29,000 \times 22}{60} = 10,630 \text{ k-in}^2/\text{in} \quad (\text{A3d})$$

$$D_b = \frac{Et_b^3}{12(1 - \mu^2)} \quad (\text{A3b})$$

$$D_b = \frac{29,000 (.562)^3}{12(1 - .3^2)} = 471 \text{ k-in}^2/\text{in}$$

$$v = \frac{\frac{1}{D_c} [(2a + b)abc] + \frac{1}{D_a} [ba^3]}{(a + b) \left[ \frac{a^3}{D_a} + \frac{2c(a^2 + ab + b^2)}{D_c} + \frac{b^3}{D_b} \right]} \quad (\text{A2})$$

$$c = 60 + 1.5 + \frac{7}{2} = 65 \text{ in.}$$

$$v = \frac{\frac{1}{10,630} \left\{ [(2 \times 100) + 80] [100 \times 80 \times 65] \right\} + \frac{1}{114,000} [80 \times 100^3]}{(100 + 80) \left[ \frac{100^3}{114,000} + \frac{2 \times 65 (100^2 + (100 \times 80) + 80^2)}{10,630} + \frac{80^3}{473} \right]}$$

$$\underline{\underline{v = .058}}$$

$$\delta_1 = \frac{ab}{24(a+b)} \left\{ \frac{c}{D_c} \left[ \frac{2ab}{a+b} - v(2a+b) \right] + \frac{a^2}{D_a} \left[ \frac{b}{a+b} - v \right] \right\} \quad (A1)$$

$$\delta_1 = \frac{100 \times 80}{24(100+80)} \left\{ \frac{65}{10,630} \left[ \frac{2 \times 100 \times 80}{100+80} - .058((2 \times 100) + 80) \right] + \frac{100^2}{114,000} \left[ \frac{80}{100+80} - .058 \right] \right\}$$

$$\delta_1 = \underline{.822 \text{ in}^2/\text{k}}$$

$$\beta = \sqrt[4]{\frac{1}{EI_c \delta_1}} \quad (A5)$$

$$\beta = \sqrt[4]{\frac{1}{29,000 \times 190,000 \times .822}} = \underline{3.84 \times 10^{-3} \text{ in}^{-1}}$$

Assume spacing of interior bracing,  $l$ , to be 25 feet for first trial.

$$\beta l = (3.84 \times 10^{-3})(25 \times 12) = \underline{1.15}$$

AASHTO Section 1.7.49 (c) (2) limits the range of transverse bending stresses to 20,000 psi. If we assume that the torque may be applied in either direction, allowable  $\sigma_t = \pm 10$  ksi. The applied torque is 2,000 k-in.

$$\sigma_t = C_t F_d \beta \frac{T}{2a} \quad (A8)$$

$$10 = C_t F_d \times .00384 \times \frac{2,000}{2 \times 100}$$

$$C_t F_d = \underline{259}$$

Calculate the section modulus,  $S_{web}$ , of the effective area of web and transverse stiffener.

$$S_{web} = \frac{I_s}{y \text{ (stiffener spacing)}} = \frac{22.0}{5.12 \times 60} = .0716 \text{ in}^3/\text{in}$$

$y$  = distance from neutral axis to extreme fiber of stiffener and effective portion of web plate

For the bottom corner of the box:

$$F_d = \frac{bv}{2S} = \frac{80 \times .058}{2 \times .053} = \underline{44 \text{ in}^{-1}} \quad (A9a)$$

$$S_{\text{bottom flange}} = \frac{1}{6} (.5625)^2 = .053 \text{ in}^3/\text{in} < .0716 \text{ in}^3/\text{in}$$

$S_{\text{bottom flange}}$  is critical at bottom corners of box.

From the top corner of the box:

$$F_d = \frac{a}{2S} \left[ \frac{b}{a+b} - v \right] \quad (A9b)$$

$$F_d = \frac{100}{2 \times .0716} \left[ \frac{80}{100+80} - .058 \right]$$

$$F_d = \underline{270 \text{ in}^{-1}}$$

Therefore, the top corners are critical, and  $S_{web}$  is used to calculate  $\sigma_t$ .

The minimum  $C_t$  can be determined as follows:

$$C_t \times 270 = 259$$

$$C_t = \underline{.956}$$

The critical point is at midpanel, with the concentrated torque also at midpanel. This can be visualized by consideration of the analogous deflection of a beam on elastic foundations. This case is treated in Figure A6. A "q" value of 1.0 is satisfactory since the point  $C_t = .956$  and  $\beta l = 1.15$  lies to the right and below  $q = 1.0$  in the figure. This value of "q" implies a nominal diaphragm is satisfactory, but axial force in the diaphragm should be checked.

**Determination of Diaphragm Brace Requirements**/Using Equation (A6), the required brace area can be calculated.

$$q = \left[ \frac{E_b A_b}{L_b l \delta_1} \right] \delta_b^2 \quad (\text{A6})$$

$$\delta_b = \frac{2(1 + a/b)}{\sqrt{1 + \left[ \frac{a+b}{2h} \right]^2}} \delta_1 \quad (\text{A7})$$

$$\delta_b = \frac{2(1 + 100/80)}{\sqrt{1 + \left[ \frac{100 + 80}{2 \times 65} \right]^2}} \times .833$$

$$\delta_b = \underline{1.285 \text{ in}^2/\text{k}}$$

$$L_b = \sqrt{90^2 + 60^2} = 108 \text{ in.}$$

Rewriting Equation (A6) with  $q = 1.0$ :

$$1.0 = \frac{29,000 A_b}{108 \times 25 \times 12 \times .822} \times 1.285^2$$

$$A_b = \underline{.556 \text{ in}^2}$$

Angles 5 x 5 x 5/16 provide the required area:  $A_b = 3.03 \text{ in}^2$ . Using this size angle, "q" is recalculated using the ratio of actual to required brace area times the required "q" value of 1.0 determined above:

$$q = \frac{1.0 \times 3.03}{.556} = \underline{5.44 \gg 1.0 \text{ OK}}$$

The force in the brace is maximum, with concentrated torque loads as close as possible to the diaphragm. The influence line in Figure A11 can be used to estimate the reaction at a rigid diaphragm for loads in adjacent panels. The torque of 2000 k-in. is due to a single rear axle of an HS truck. Adjacent front axle and rear axles produce torques of 400 k-in. and 2000 k-in. respectively, each 14 feet from the diaphragm. The equivalent torque is found by using the influence line coefficients from Figure A11.

$$2000 [1 + (1 + .25) (.51)] = \underline{3275 \text{ k-in.}}$$

From Figure A10,  $C_b$  is approximately equal to 0.6 for  $q = 5.44$ . The brace force,  $F_b$ , may be calculated using Equation (A11):

$$F_b = C_b \left[ \frac{\sqrt{1 + \left( \frac{a+b}{2h} \right)^2}}{2 \left( 1 + \frac{a}{b} \right)} \right] \frac{(T)}{a} \quad (\text{A11})$$

$$F_b = 0.6 \left[ \frac{\sqrt{1 + \left( \frac{100 + 80}{2 \times 65} \right)^2}}{2 \left( 1 + \frac{100}{80} \right)} \right] \frac{(3275)}{100}$$

$$F_b = \underline{7.47 \text{ kips}}$$

$$A_b = 3.03 \text{ in}^2$$

$$\sigma_b = \frac{7.47}{3.03} \times 1000 = \underline{2,470 \text{ psi}}$$

Since the braces are assumed effective in compression, the compression stress must be checked.

From AASHTO, the allowable compression stress is:

$$\sigma_{\text{allowable}} = 16,980 - .53 \left( \frac{KL_b}{r} \right)^2$$

$$= 16,980 - .53 \left( \frac{108}{.994} \right)^2$$

$$= \underline{10,723 \text{ psi} \gg 2,470 \text{ psi OK}}$$

The calculated maximum stress range is  $2 \times 2.47 = 4.94 \text{ ksi}$ . This is within allowable AASHTO fatigue stress of 5 ksi for 2,000,000 cycles for Category E, so the braces could be welded. If higher stresses occur, bolted connections would be required.

### Determination of Normal Distortional Stress/

Normal stress is generally largest at midpanel, with the concentrated torque applied at midpanel. This stress is analogous to moment in a beam on elastic foundation. If the diaphragm stiffness is low ( $q < 10$ ), the critical condition may occur at the diaphragm with the concentrated torque at the same location. This situation can occur only when  $\beta l$  is very small ( $\beta l < 1$ ), and is not a practical design situation.

The normal distortional stress is determined using Equation (A10) and Figure A9 for concentrated torque:

$$\sigma_{dw} = \frac{C_w y}{I \beta a} [T] \quad (\text{A10})$$

$C_w$  is found to be 0.8 for  $\beta = 1.15$  and  $q = 5.44$

$$\sigma_{dw} = \frac{0.80(y)}{1.9 \times 10^5 \times 3.84 \times 10^{-3} \times 100} (2000)$$

$$\sigma_{dw} = .0219 y$$

$$y_{\text{bottom}} = \underline{49.59 \text{ in.}} \quad y_{\text{top steel}} = \underline{10.41 \text{ in.}}$$

The critical condition is at the bottom of the box.

$$\sigma_{dw} = .0219 \times 49.59 = \underline{1.09 \text{ ksi}}$$

The normal distortional stress is added to the bending stresses produced by the critical torsional condition. Often, the critical maximum bending stresses are produced by different positions of live load.

## References

1. Abdel-Samad, S. R., Wright, R. N., "Analysis of Box Girders with Diaphragms," *Journal of the Structural Division*, ASCE, Vol. 94, No. ST 10, Oct., 1968.
2. *American Association of State Highway and Transportation Officials Standard Specifications for Highway Bridges*, 12th Edition, 1977.
3. *Analysis of Curved Folded Plate Structures*, Report No. UC SESM 70-8, University of California, Berkeley, Calif., June, 1970.
4. Dabrowski, R., *Curved Thin Walled Girders*, Cement and Concrete Association, London, England, 1968.
5. Dowling, P. J., "Strength of Steel Box-Girder Bridges," *Journal of the Structural Division*, ASCE, Vol. 101, No. ST 9, Sept., 1975.
6. Fam, A. R. M., *Static and Free Vibration Analyses of Curved Box Bridges*, PhD Thesis, McGill University, Montreal, Canada, Dec., 1972.
7. Hall, D. H. et al, "Curved Steel Box-Girder Bridges: A Survey," *Journal of the Structural Division*, ASCE, Vol. 104, No. ST 11, Nov., 1978.
8. Hall, D. H. et al, "Curved Steel Box-Girder Bridges: State of the Art," *Journal of the Structural Division*, ASCE, Vol. 104, No. ST 11, Nov., 1978.
9. Heins, C. P., Kuo, J. T. C., Torsional Properties of Composite Girders, *AISC Engineering Journal*, Vol. 19, No. 2, April, 1972.
10. Heins, C. P., Kuo, J. T. C., "Composite Beams in Torsion," *Journal of the Structural Division*, ASCE, Vol. 98, No. ST 5, May, 1972.
11. Heins, C. P., Blank, D., *Box Beam Stiffening Using Cold-Formed Decks*, Second Specialty Conference on Cold Formed Steel Structures, Oct. 22-24, St. Louis, Mo., 1973, pp. 537-571.
12. Heins, C. P., *Bending and Torsional Design of Structural Members*, Lexington Books, Lexington, Massachusetts, 1975.
13. Heins, C. P., Olenik, J. C., "Curved Box Beam Bridge Analysis," *Computers and Structures Journal*, Vol. 6, Pergamon Press, London, 1976, pp. 65-73.
14. Heins, C. P., *AD-BOXGD—Analysis and Design of Box Girders Straight and Curved for Highway and Rapid Rail Systems*, Users Manual, Civil Engineering Dept., University of Maryland, College Park, Md., Sept., 1978.
15. *Manual of Bridge Design*, State of California Dept. of Public Works, Division of Highways, Bridge Dept., Sacramento, Calif., 1971.
16. Mattock, A. H., Johnston, S. B., *An Experimental and Analytical Study of the Lateral Distribution of Load in Composite Box Girder Bridges, Final Report*, U.S.S. Corp., Pittsburgh, Pa., 1968.
17. Mattock, A. H., "Development of Design Criteria for Composite Box Girder Bridges," *Developments in Bridge Design and Construction*, Crosby Lockwood & Sons, London, England, Nov., 1971.
18. McDonald, R. E., Chen, Y. S., Yilmaz, C., Yen, B. T., "Open Steel Box Sections with Top Lateral Bracing," *Journal of the Structural Division*, ASCE, Vol. 102, No. ST 1, January, 1975.
19. Moffatt, K. R., Dowling, P. J., *Steel Box Girders Parametric Study on the Shear Lag Phenomenon in Steel Box Girder Bridges*, Engineering Structures Laboratory, Civil Engineering Dept., Imperial College, London, CESLIC Report BG 17, September, 1972.
20. Mozer, J. D., Culver, C. G., "Behavior of Curved Box Girders—Laboratory Observations," *ASCE Specialty Conference on Metal Bridges*, St. Louis, Mo., Nov. 12-13, 1974.
21. Nakai, H., Heins, C. P., "Analysis Criteria for Curved Bridges," *Journal of the Structural Division*, Vol. 103, No. ST 7, July, 1977.
22. Olenik, J. C., Heins, C. P., *Diaphragm Spacing Requirements for Curved Steel Box Beam Bridges*, Civil Engineering Report No. 58, University of Maryland, College Park, Md., August, 1974.
23. Olenik, J. C., Heins, C. P., "Diaphragms for Curved Box Beam Bridges," *Journal of the Structural Division*, Vol. 101, No. ST 10, Oct., 1975.
24. *Tentative Design Specifications for Horizontally Curved Highway Bridges, Final Report, CURT Project HPR2-(111)*, March, 1975.
25. Timoshenko, S. P., Gere, J. M., *Theory of Elastic Stability*, 2nd Ed., McGraw-Hill, New York, 1961.
26. *Users Manual for the Static Analysis of Curved Bridges (STACRB)*, Report No. T0173, Civil Engineering Dept., University of Pennsylvania, Philadelphia, Pa., June, 1973.

27. Vlasov, V. Z., *Thin Walled Beam Theory*, NSF, Washington, D.C., 1961.
28. Walsh, D., Heins, C. P., *Distribution Factors for Curved Box Girders*, CE Report, University of Maryland, College Park, Md., June, 1977.
29. Williamson, D. M., *BEF Analysis for Cross-Sectional Deformation of Curved Box Girders with Internal Diaphragms*, M. S. Thesis, CE Dept., Carnegie-Mellon University, Pittsburgh, Pa., April, 1974.
30. Wright, R. N., Abdel-Samad, S. R., Robinson, A. R., *Analysis and Design of Closed-section Girder Bridges with Diaphragms, Final Report to AISI, Project 110*, Dept. of Civil Engineering, University of Illinois, March, 1967.
31. Wright, R. N., Abdel-Samad, S. R., "BEF Analogy for Analysis of Box Girders," *Journal of the Structural Division*, ASCE, Vol. 94, No. ST 7, July, 1968.